Does the gamma-ray signal from the central Milky Way indicate Sommerfeld enhancement of dark matter annihilation?

Man-Ho Chan

Department of Science and Environmental Studies, The Education University of Hong Kong, Tai Po, New Territories, Hong Kong, China

Abstract   Recently, some studies showed that the GeV gamma-ray excess signal from the central Milky Way can be explained by the annihilation of ~ 40 GeV dark matter through the $b\bar{b}$ channel. Based on the morphology of the gamma-ray flux, the best-fit inner slope of the dark matter density profile is $\gamma = 1.26$. However, recent analyses of the Milky Way dark matter profile favor $\gamma = 0.6 - 0.8$. In this article, we show that the GeV gamma-ray excess can also be explained by the Sommerfeld-enhanced dark matter annihilation through the $b\bar{b}$ channel with $\gamma = 0.85 - 1.05$. We constrain the parameters of the Sommerfeld-enhanced annihilation by using data from Fermi-LAT. We also show that the predicted gamma-ray fluxes emitted from dwarf galaxies generally satisfy recent upper limits on gamma-ray fluxes detected by Fermi-LAT.

Key words: (cosmology): dark matter

1 INTRODUCTION

In the past few years, some excess GeV gamma rays emitted from our Galactic center were reported (Hooper & Slatyer 2013; Huang et al. 2013; The Fermi-LAT Collaboration 2015). The large diffuse signal of GeV gamma rays is hard to explain by cosmic ray and pulsar emission. Recent studies point out that millisecond pulsars can only account for no more than 10% of the GeV excess (Hooper et al. 2013; Daylan et al. 2016). Therefore, the possibility of emission of gamma rays due to dark matter annihilation has become a hot topic in recent years (Daylan et al. 2016; Gordon & Macías 2013; Abazajian et al. 2014; Izaguirre et al. 2014; Calore et al. 2015).

In particular, Daylan et al. (2016); Calore et al. (2015) discovered that the gamma-ray spectrum obtained from Fermi-LAT can be well fitted with $m = 30 - 70$ GeV dark matter annihilation through the $b\bar{b}$ channel. The cross section obtained, $\langle \sigma v \rangle = (1.4 - 2.0) \times 10^{-26}$ cm^3 s^{-1}, generally agrees with the expected canonical thermal relic abundance cross section $\langle \sigma v \rangle \approx (2 - 3) \times 10^{-26}$ cm^3 s^{-1}. Moreover, the inner slope of the radial-dependence of the gamma-ray emission is $\gamma \approx 1.1 - 1.3$ (the best-fit value is $\gamma = 1.26$), which is consistent with the theoretical expectation from numerical simulations ($\gamma = 1 - 1.5$) (Daylan et al. 2016). This work is further supported by a later study which includes consideration of foreground and background uncertainties (Calore et al. 2015). On the other hand, Chan (2015) showed that this dark matter model can also explain the origin of hot gas near the Galactic center.

Therefore, this dark matter model has become one of the most popular models in dark matter astrophysics.

Besides the detection of gamma-ray emission from the Galactic center, Fermi-LAT data were also used to obtain some upper limits on gamma-ray emission from dwarf galaxies and galaxy clusters. If we assume that the gamma-ray emission is due to annihilation of $m = 40$ GeV dark matter through the $b\bar{b}$ channel, the corresponding upper limits on cross sections are $\langle \sigma v \rangle \approx 1 \times 10^{-26}$ cm^3 s^{-1} (Ackermann et al. 2014, 2015) and $\langle \sigma v \rangle \approx (2 - 3) \times 10^{-25}$ cm^3 s^{-1} (Ando & Nagai 2012) for dwarf galaxies and galaxy clusters respectively.

In fact, the results obtained in Daylan et al. (2016); Calore et al. (2015) assume that the annihilation cross section is constant (velocity-independent). However, it has been suggested that the annihilation cross section can be velocity-dependent. For example, the multiple exchange of some light force-carrier particle between the annihilating dark matter particle (the Sommerfeld enhancement) gives $\langle \sigma v \rangle \propto v^{-\alpha}$, where $\alpha = 1$ and $\alpha = 2$ are for non-resonance and resonance respectively (Sommerfeld 1931; Zavala et al. 2010; Yang et al. 2014). Furthermore, the inner slope of dark matter in our Galactic center revealed in Daylan et al. (2016); Calore et al. (2015) (best-fit $\gamma = 1.26$) is a bit too large compared with the recent observations of the Milky Way (Pato et al. 2015). Recent studies point out that the Milky Way dark matter density is well-fitted by a Navarro-Frenk-White (NFW) density profile ($\gamma = 1$) (Navarro et al. 1997; Iocco et al. 2015;

Pato et al. 2015). Detailed analyses in Pato et al. (2015) show that the best-fit 2σ range of the inner slope for the most representative baryonic model is $\gamma = 0.6 - 0.8$. If we assume a generalized NFW profile with local density $\rho_\odot = 0.4\ \text{GeV cm}^{-3}$, $\gamma > 1.2$ is excluded (outside the 5σ region) for this representative baryonic model. Although these results do not really rule out the possibility of having $\gamma = 1.1 - 1.3$ (some baryonic models can still generate these values), such a large inner slope in the Milky Way is certainly questionable. In fact, most of the inner slopes of dark matter density profiles observed do not show $\gamma > 1$. For example, most galaxy clusters give $\gamma \approx 1$ (Pointecouteau et al. 2005) and most galaxies and dwarf galaxies give $\gamma \leq 1$ (Salucci 2001; Oh et al. 2011; Loeb & Weiner 2011). Furthermore, recent numerical simulations show that baryonic feedback can decrease the inner slope of dark matter such that $\gamma < 1$ for normal galaxies (Governato et al. 2012; Pontzen & Governato 2014). Therefore, the inner slope obtained in Daylan et al. (2016); Calore et al. (2015) does not give a good agreement with many other observations and recent numerical simulations.

In this article, we show that the result obtained in Daylan et al. (2016) is completely compatible with a velocity-dependent annihilation cross section. If we assume that the dark matter annihilation in the Milky Way's center is Sommerfeld-enhanced, then the resulting inner slope γ obtained would give $\gamma = 0.85 - 1.05$, which agrees with the standard NFW profile ($\gamma = 1$). Also, we show that our model satisfies the Fermi-LAT results of nearby dwarf galaxies.

2 THE POSSIBILITY OF SOMMERFELD ENHANCEMENT

The observed gamma-ray flux within a solid angle $\Delta\Omega$ due to dark matter annihilation can be calculated by

$$\phi(\Delta\Omega) = \frac{\langle\sigma v\rangle}{8\pi m^2} \int \frac{dN_\gamma}{dE} dE \int_{\Delta\Omega} d\Omega \int_{\text{los}} \rho^2 ds, \quad (1)$$

where dN_γ/dE is the photon spectrum per one dark matter annihilation (see Fig. 1) (Cembranos et al. 2011) and ρ is the dark matter density. The above equation is usually expressed as $\phi = \phi_{pp} J$, where

$$\phi_{pp} = \frac{\langle\sigma v\rangle}{8\pi m^2} \int \frac{dN_\gamma}{dE} dE \quad (2)$$

is known as the 'particle-physics factor' and

$$J = \int_{\Delta\Omega} d\Omega \int_{\text{los}} \rho^2 ds \quad (3)$$

is known as the J-factor.

Generally speaking, the best-fit annihilation channel, rest mass and annihilation cross section of a dark matter particle can be determined by the value of ϕ and the observed energy spectrum. In the above expressions, the annihilation cross section is assumed to be a constant.

Therefore, only the integrand of the J-factor depends on r. However, if the annihilation cross section is velocity-dependent, Equation (1) has to be revised to include the effect of dark matter velocity.

We assume that the annihilation cross section is generally given by $\langle\sigma v\rangle = \langle\sigma v\rangle_0 (v_0/v)^\alpha$, where v is the velocity dispersion of dark matter particles, and v_0 and $\langle\sigma v\rangle_0$ are constant. For the Sommerfeld enhancement, we have $\alpha \approx 1$ or $\alpha \approx 2$ for non-resonance and resonance cases respectively (Yang et al. 2014). By putting the velocity-dependent cross section into Equation (1), we can rewrite the particle-physics factor and J-factor respectively as

$$\phi'_{pp} = \frac{\langle\sigma v\rangle_0}{8\pi m^2} \int \frac{dN_\gamma}{dE} dE \quad (4)$$

and

$$J' = \int_{\Delta\Omega} d\Omega \int_{\text{los}} \rho^2 \left(\frac{v_0}{v}\right)^\alpha ds. \quad (5)$$

Recent observations indicate that the dark matter density profile in our Galaxy is very close to an NFW profile (Iocco et al. 2015). Therefore, for a region with small r ($r \leq 5$ kpc), we assume that $\rho = \rho_s(r/r_s)^{-1}$, where ρ_s and r_s are the scale density and scale radius respectively. The mass profile of the dark matter halo is $M_d = 2\pi\rho_s r_s r^2$. Since dark matter forms structure earlier than baryons, in an equilibrium configuration, the velocity dispersion of dark matter follows $v = C\sqrt{GM_d/r}$, where $C \sim 1$ is a constant which depends on the structure of the halo (Nesti & Salucci 2013). However, most of the data on observed morphology have been obtained in the region $r \sim 1$ kpc (Calore et al. 2015). When baryons collapse and form structures, the total mass of this small region would be dominated by the bulge mass. Although we know that the infall of baryons and some of the baryonic processes would affect the density distribution of dark matter, it is still not very clear quantitatively how this process affects the dark matter distribution and velocity distribution in our Galaxy. Recent numerical simulations indicate that this effect is mainly determined by the ratio of stellar mass to the dark halo mass. Based on the study in Di Cintio et al. (2014), the dark matter distribution of a Milky Way-size galaxy approaches the NFW profile for $r \sim 1$ kpc. However, based on consideration of angular momentum, the velocity of dark matter particles would still change due to baryonic infall (adiabatic contraction). This would change the anisotropy coefficient β, which depends on the ratio of the tangential and radial velocities of dark matter particles. The analytic calculations in Vasilev (2006) show that if the change in the anisotropy coefficient is not very large, in some models, the velocity dispersion still follows the original NFW velocity distribution profile $v \propto \sqrt{r}$. In the following, although the mass profile is dominated by the bulge mass at $r \sim 1$ kpc, we assume that the distribution of dark matter and its velocity dispersion approximately follows the original NFW profile. In other words, we assume

that the velocity distribution of dark matter is the same as the dark matter-only case, i.e. $v = C\sqrt{2\pi G \rho_s r_s r}$ [1]. Even if the resulting velocity distribution deviates significantly from the original one, the numerical factor C can also reflect some of the deviation in the following calculations. Based on the above assumption, we have

$$J' = \int_{\Delta\Omega} d\Omega \int_{\text{los}} \rho^2 \left(\frac{r_0}{r}\right)^{\alpha/2} ds, \qquad (6)$$

where $r_0 = v_0^2 / 2\pi G C^2 \rho_s r_s$.

Since the Sommerfeld enhancement does not affect the energy spectrum of gamma rays in terms of dN_γ/dE, the best-fit annihilation channel and rest mass of dark matter particles in Daylan et al. (2016) would not be changed. The only parameter that changes is the annihilation cross section. Based on the total gamma-ray flux detected, the velocity-dependent cross section can be constrained by

$$\phi = \phi_{pp} J = \phi'_{pp} J'. \qquad (7)$$

Technically, the Fermi-LAT observation is able to express the emission of gamma-ray flux as a function of r ($F(r) \propto r^{-2\gamma}$) (Daylan et al. 2016). This function is directly proportional to the integrand of J. Therefore, to be consistent with the observed morphology, the integrand of J and J' must have the same r-dependence

$$\rho_s^2 \left(\frac{r_s}{r}\right)^2 \left(\frac{r_0}{r}\right)^{\alpha/2} = \rho_s'^2 \left(\frac{r_s}{r}\right)^{2\gamma}, \qquad (8)$$

where ρ'_s is the scale density used in Daylan et al. (2016). By using the best-fit value $\gamma = 1.26$ (Daylan et al. 2016), we get $\alpha = 2(2\gamma - 2) = 1.04 \approx 1$. In other words, the result obtained in Daylan et al. (2016) can also be interpreted as a non-resonant Sommerfeld-enhanced dark matter annihilation with an NFW dark matter density profile ($\gamma = 1$). If we fix $\alpha = 1$ and release the inner slope of dark matter density γ to be a free parameter, then the morphology of the gamma-ray flux $F(r) \propto r^{-(2.2-2.6)}$ from observations (Daylan et al. 2016) would give $\gamma = 0.85 - 1.05$, which is close to the 2σ region ($\gamma = 0.4 - 1$) for the most representative baryonic model (Pato et al. 2015).

Based on the above formalism, we can obtain the value of $\langle\sigma v\rangle_0 v_0$ by using the flux ϕ. By assuming $C = 1$, $\gamma = 1$, $r_s = 20$ kpc and the local dark matter density $\rho_\odot = 0.4$ GeV cm^{-3} (Iocco et al. 2015), we get $\langle\sigma v\rangle_0 v_0 \approx (2.2 - 3.2) \times 10^{-19}$ cm^4 s^{-2}.

3 SOMMERFELD ENHANCEMENT IN DWARF GALAXIES

If the Sommerfeld enhancement of dark matter annihilation occurs in our Galaxy, then the same situation would
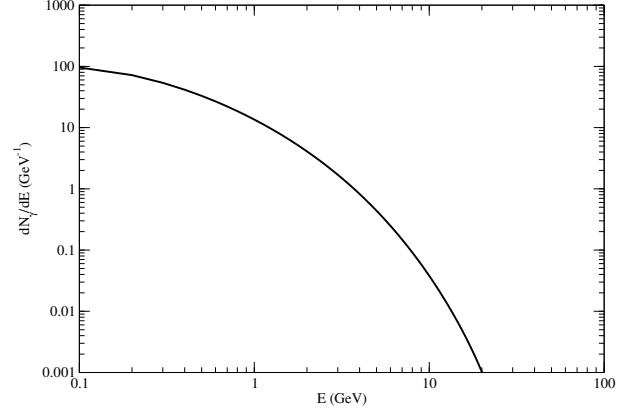
Fig. 1 The photon spectrum per one dark matter annihilation through the $b\bar{b}$ channel (Cembranos et al. 2011). Here, we assume $m = 40$ GeV.

also occur in dwarf galaxies. In fact, the velocity dispersion near the center of a dwarf galaxy is small ($v \sim 10$ km s^{-1}). This small velocity dispersion would give a large annihilation rate near the centers of dwarf galaxies.

From the result in Ackermann et al. (2015), the upper limit of annihilation cross section for the $b\bar{b}$ channel from the stacked analysis is $\langle\sigma v\rangle \sim 2 \times 10^{-26}$ cm^3 s^{-1} for $m \leq 70$ GeV. However, if we include the effect of the Sommerfeld enhancement, then we need to replace the J-factors used in Ackermann et al. (2014, 2015) by Equation (6). Moreover, the J-factors used in Ackermann et al. (2014, 2015) are somewhat larger than those in recent empirical fits (Bonnivard et al. 2015; Evans et al. 2016). Therefore, in the following, we use the lower limit of the J-factor for each dwarf galaxy in Bonnivard et al. (2015); Evans et al. (2016) and calculate a conservative upper limit of $\langle\sigma v\rangle_0 v_0$ based on the likelihood analysis in Ackermann et al. (2015).

Following Evans et al. (2016), the J-factor of a dwarf galaxy can be given by an analytic formula

$$J(\gamma) = \frac{25\sigma_{\text{los}}^4}{64G^2} \frac{1}{D^2 R_{\text{h}}} \left(\frac{D\theta}{R_{\text{h}}}\right)^{3-2\gamma} P(\gamma), \qquad (9)$$

where

$$P(\gamma) = \frac{2}{\pi^{1/2}} \frac{(3-\gamma)^2 \Gamma(\gamma - 0.5)}{(3 - 2\gamma)\Gamma(\gamma)}, \qquad (10)$$

σ_{los} is the velocity dispersion, D is the distance to the galaxy, $\theta = 0.5°$ is the angular size and R_{h} is the projected half-light radius (Evans et al. 2016). By using Equation (6) and assuming $\gamma = 1$ and $\alpha = 1$, the revised J-factor for the Sommerfeld enhancement is given by

$$J' = J(1) \left(\frac{r_0}{D\theta}\right)^{1/2} \frac{P(1.25)}{P(1)}. \qquad (11)$$

Table 1 The Lower Limits of the Sommerfeld-enhanced J-factors J' for Different Dwarf Galaxies

Dwarf galaxy	$\log(J'/\mathrm{GeV^2\ cm^{-5}})$
Boötes I	17.0
Canes Venatici II	17.6
Carina	18.2
Coma Berenices	19.1
Draco	19.3
Fornax	18.2
Hercules	16.9
Leo II	17.6
Leo IV	13.4
Sculptor	19.0
Segue I	13.5
Sextans	17.9
Ursa Major II	19.8
Ursa Minor	19.2
Willman 1	18.5
Canes Venatici I	17.6
Leo I	17.8
Ursa Major I	18.7

By using the lower limits of the J-factor obtained in Bonnivard et al. (2015); Evans et al. (2016), the combined revised J-factor is 2.3 times the original combined J-factor obtained in Ackermann et al. (2015) (see Table 1 for the Sommerfeld-enhanced lower limit of the J-factor for each dwarf galaxy). Therefore, the results in Ackermann et al. (2015) would make the upper limit of $\langle\sigma v\rangle_0 v_0$ be 2×10^{-19} cm^4 s^{-2}, which is close to our range of $\langle\sigma v\rangle_0 v_0 = (2.2 - 3.2) \times 10^{-19}$ cm^4 s^{-2}. Nevertheless, recent studies suggest that the dark matter density profiles of dwarf galaxies are cored profiles ($\gamma < 1$) instead of $\gamma = 1$ (de Blok et al. 2003; Spekkens et al. 2005; Oh et al. 2011; Burkert 2015). Therefore, the upper limit would be a bit larger because we have used the NFW profile ($\gamma = 1$) to model the dark matter density profile of the dwarf galaxies. As estimated by Ackermann et al. (2015), this can give a factor of 1.3 in the upper limit. Also, if the inner density profiles of dwarf galaxies are cored, then the value of C in dwarf galaxies may be a factor of 2 larger than that of the Milky Way (Nesti & Salucci 2013). As a result, if we include all the above mentioned factors, the corresponding upper limit of $\langle\sigma v\rangle_0 v_0$ would be larger by a factor of 1.8 (i.e. $\langle\sigma v\rangle_0 v_0 \leq 3.6 \times 10^{-19}$ cm^4 s^{-2}) and it would agree with the range observed by Fermi-LAT for the Milky Way. This means that the Sommerfeld-enhanced gamma-ray flux in dwarf galaxies does not exceed the observed upper limit.

4 DISCUSSION

Previously, Daylan et al. (2016) showed that the GeV gamma-ray excess can be explained by annihilation of ~ 40 GeV dark matter through the $b\bar{b}$ channel. Based on the morphology of the gamma-ray flux, the best-fit in-

ner slope of the dark matter density profile is $\gamma = 1.26$. However, recent analyses show that the best-fit 2σ range of the inner slope for the most representative baryonic model is $\gamma = 0.6 - 0.8$ (Pato et al. 2015). In addition, many observations indicate $\sigma \leq 1$ (Salucci 2001; Oh et al. 2011; Loeb & Weiner 2011). In this article, we show that the GeV gamma-ray excess can also be explained by the Sommerfeld-enhanced dark matter annihilation through the $b\bar{b}$ channel with $\gamma = 1$ (the NFW profile). In general, our model is compatible with the range of inner slope $\gamma = 0.85 - 1.05$. By using the results in Daylan et al. (2016), we also constrain the parameters of the Sommerfeld enhancement: $\alpha = 1$ and $\langle\sigma v\rangle_0 v_0 \approx (2.2 - 3.2) \times 10^{-19}$ cm^4 s^{-1} for $\gamma = 1$.

Although the annihilation model with a Sommerfeld enhanced cross section is more complicated, this model can fully explain the morphology of the gamma-ray flux and favor the smaller inner slope of the dark matter density in the Milky Way. Since the morphology of the gamma-ray flux gives $F \propto r^{-(2.2-2.6)}$ (Daylan et al. 2016), the inner slope obtained from this model is $\gamma = 0.85 - 1.05$, which agrees very well with the recent analysis in Pato et al. (2015). However, if we assume a constant cross section for dark matter annihilation, then the required inner slope is $\gamma = 1.1 - 1.3$, which is not consistent with the observed 2σ range of the inner slope $\gamma = 0.6 - 0.8$ for the most representative baryonic model (Pato et al. 2015). Therefore, our model can alleviate the tension between the existing dark matter annihilation model and observations.

In fact, the Sommerfeld enhancement would greatly enhance the dark matter annihilation rate near the center of a dwarf galaxy because the velocity dispersion is very small there. Therefore, we predict that a strong signal of gamma-ray flux at the center of a dwarf galaxy would result if our model is correct. We show that the gamma-ray fluxes emitted due to Sommerfeld-enhanced dark matter annihilation from dwarf galaxies generally agree with the current upper limits obtained by the 6-year Fermi-LAT data. If Fermi-LAT data can be used to further constrain the upper limits on gamma-ray flux or the detected gamma-ray spectrum in the future, then we can get a tighter constraint on the annihilation cross section as well as the rest mass of dark matter.

References

Abazajian, K. N., Canac, N., Horiuchi, S., & Kaplinghat, M. 2014, Phys. Rev. D, 90, 023526

Ackermann, M., Albert, A., Anderson, B., et al. 2014, Phys. Rev. D, 89, 042001

Ackermann, M., Albert, A., Anderson, B., et al., [Fermi-LAT Collaboration], 2015, Physical Review Letters, 115, 231301

Ando, S., & Nagai, D. 2012, J. Cosmol. Astropart. Phys., 7, 017

Bonnivard, V., Combet, C., Daniel, M., et al. 2015, MNRAS, 453, 849

Burkert, A. 2015, ApJ, 808, 158

Calore, F., Cholis, I., McCabe, C., & Weniger, C. 2015, Phys. Rev. D, 91, 063003

Cembranos, J. A. R., de La Cruz-Dombriz, A., Dobado, A., Lineros, R. A., & Maroto, A. L. 2011, Phys. Rev. D, 83, 083507

Chan, M. H. 2015, MNRAS, 448, L87

Daylan, T., Finkbeiner, D. P., Hooper, D., et al. 2016, Physics of the Dark Universe, 12, 1 (arXiv:1402.6703)

de Blok, W. J. G., Bosma, A., & McGaugh, S. 2003, MNRAS, 340, 657

Di Cintio, A., Brook, C. B., Macciò, A. V., et al. 2014, MNRAS, 437, 415

Evans, N. W., Sanders, J. L., & Geringer-Sameth, A. 2016, Phys. Rev. D, 93, 103512

Gordon, C., & Macías, O. 2013, Phys. Rev. D, 88, 083521

Governato, F., Zolotov, A., Pontzen, A., et al. 2012, MNRAS, 422, 1231

Hooper, D., Cholis, I., Linden, T., Siegal-Gaskins, J. M., & Slatyer, T. R. 2013, Phys. Rev. D, 88, 083009

Hooper, D., & Slatyer, T. R. 2013, Physics of the Dark Universe, 2, 118

Huang, W.-C., Urbano, A., & Xue, W. 2013, arXiv:1307.6862

Iocco, F., Pato, M., & Bertone, G. 2015, Nature Physics, 11, 245

Izaguirre, E., Krnjaic, G., & Shuve, B. 2014, Phys. Rev. D, 90, 055002

Loeb, A., & Weiner, N. 2011, Physical Review Letters, 106, 171302

Navarro, J. F., Frenk, C. S., & White, S. D. M. 1997, ApJ, 490, 493

Nesti, F., & Salucci, P. 2013, J. Cosmol. Astropart. Phys., 7, 016

Oh, S.-H., de Blok, W. J. G., Brinks, E., Walter, F., & Kennicutt, Jr., R. C. 2011, AJ, 141, 193

Pato, M., Iocco, F., & Bertone, G. 2015, J. Cosmol. Astropart. Phys., 12, 001

Pointecouteau, E., Arnaud, M., & Pratt, G. W. 2005, A&A, 435, 1

Pontzen, A., & Governato, F. 2014, Nature, 506, 171

Salucci, P. 2001, MNRAS, 320, L1

Sommerfeld, A. 1931, Annalen der Physik, 403, 257

Spekkens, K., Giovanelli, R., & Haynes, M. P. 2005, AJ, 129, 2119

The Fermi-LAT Collaboration 2015, arXiv:1511.02938

Vasilev, E. A. 2006, JETP Letters, 84, 45

Yang, L. F., Silk, J., Szalay, A. S., et al. 2014, Phys. Rev. D, 89, 063530

Zavala, J., Vogelsberger, M., & White, S. D. M. 2010, Phys. Rev. D, 81, 083502